Cosmology of Sub-MeV Dark Matter Freeze-In

Cora Dvorkin,[1,*] Tongyan Lin,[2,†] and Katelin Schutz[3,4,‡]
[1]*Department of Physics, Harvard University, Cambridge, Massachusetts 02138, USA*
[2]*Department of Physics, University of California, San Diego, California 92093, USA*
[3]*Center for Theoretical Physics, Massachusetts Institute of Technology, Cambridge, Massachusetts 02139, USA*
[4]*Department of Physics & McGill Space Institute, McGill University, Montréal, Québec, H3A 2T8, Canada*

(Received 29 November 2020; revised 27 April 2021; accepted 9 August 2021; published 9 September 2021)

Dark matter (DM) could be a relic of freeze-in through a light mediator, where the DM is produced by extremely feeble, IR-dominated processes in the thermal standard model plasma. In the simplest viable models with DM lighter than 1 MeV, the DM has a small effective electric charge and is born with a nonthermal phase-space distribution. This DM candidate would cause observable departures from standard cosmological evolution. In this work, we combine data from the cosmic microwave background (CMB), Lyman-α forest, quasar lensing, stellar streams, and Milky Way satellite abundances to set limits on freeze-in DM masses up to $\sim$20 keV, with the exact constraint depending on whether the DM thermalizes in its own sector. We perform forecasts for the CMB-S4 experiment, the Hydrogen Epoch of Reionization Array, and the Vera Rubin Observatory, finding that freeze-in DM masses up to $\sim$80 keV can be explored.

DOI: 10.1103/PhysRevLett.127.111301

Introduction.—Despite the abundant evidence of dark matter (DM) in our Universe, its properties and early-universe origins remain open questions. If DM is a particle, it may arise from thermal processes in the primordial plasma in the first moments after the Big Bang. In the scenario known as *freeze-in*, DM is produced from the annihilation or decay of standard model (SM) particles in the early universe [1–6]. As the Universe cools, the interactions that make DM become inefficient, yielding a fixed DM relic density that is observed today.

If the DM and the force-carrier particle that mediates freeze-in are sufficiently light, then the rate for SM particles to produce DM via an s-wave process must scale like $\Gamma \sim g_\chi^2 g_{\rm SM}^2 T$ for a relativistic plasma of temperature T, where g_χ is the DM-mediator coupling and $g_{\rm SM}$ is the SM-mediator coupling. Meanwhile, the Hubble rate scales like $H \sim T^2/M_{\rm Pl}$, where $M_{\rm Pl}$ is the Planck mass. This scaling indicates that freeze-in will predominantly occur at the lowest kinematically accessible temperatures, meaning that in the absence of additional interactions, the DM abundance produced during freeze-in is independent of initial conditions. Producing the observed DM abundance implies a tiny value for the coupling constants that is difficult to target with accelerator searches. However, the light mediator enhances the signal of this candidate in direct-detection experiments, since scattering via a light mediator scales like v^{-4} for velocity v, which is $v \sim 10^{-3}c$ at the Earth's location in the Milky Way (MW). In the light-mediator regime, the requisite DM-SM couplings for the observed DM abundance provide a predictive benchmark for sub-GeV DM direct-detection experiments [7–25].

There are strong stellar emission and fifth force constraints on most light mediators coupled to the SM [26,27]. The only light mediators that can be responsible for freeze-in of sub-MeV DM are the SM photon or an ultralight kinetically mixed dark photon. Thus, sub-MeV DM made by freeze-in will effectively have a small electromagnetic charge, $Q = g_\chi g_{\rm SM}/e \sim 10^{-11}$, defined relative to the electron charge e. Freeze-in is the simplest allowed way to make charged DM, since the charges required for DM production via freeze-out are excluded by many orders of magnitude [28]. Charged DM has recently been the subject of keen interest in the context of the anomalous observation by the Experiment to Detect the Global EoR Signature (EDGES) [29–31] and can also play a role in energy loss from stellar and supernova environments [32–34] and gas clouds [35,36], as well as potentially leading to novel plasma behavior in galaxies and clusters [37–42]. The scenario involving a dark photon is also of theoretical interest, as ultralight bosons are generically expected in various string theories [43,44].

Because of the extraordinarily small couplings involved, freeze-in DM never achieves a thermal number density in the early universe. This means that freeze-in is one of the few allowed ways of making sub-MeV DM from the SM thermal bath. Most other mechanisms to produce sub-MeV DM from the thermal bath are excluded (there are some exceptions, see, e.g., Refs. [45–47]) because sub-MeV DM would carry substantial energy and entropy density which would observably alter the effective number of relativistic degrees of freedom, $N_{\rm eff}$, and Big Bang Nucleosynthesis (BBN) (see, e.g., Refs. [26,27,48–50]). Note that ultralight dark photon mediators are not produced abundantly by the

SM bath in the early universe because of an in-medium suppression of the coupling [51].

Sub-MeV freeze-in via an ultralight vector mediator poses a well-motivated DM theory with a complete and consistent early-universe thermal history and a host of concrete predictions for observable phenomena. In this Letter, we explore the effects of this production mechanism on the subsequent cosmology, focusing on two key effects: (i) the portal responsible for creating the DM necessarily implies a drag force between the DM and the photon-baryon fluid before and during recombination, altering anisotropies seen in the cosmic microwave background (CMB) and (ii) the DM is born with a nonthermal, high-velocity phase-space distribution, which suppresses clustering on small scales. We constrain the former effect with the *Planck* 2018 CMB power spectra and show how the bound can improve with the CMB-S4 experiment. We constrain the latter effect with the Lyman-α forest, strong gravitational lensing of quasars, stellar streams, and MW satellites. We additionally forecast the DM masses that can be explored with observations of the 21 cm power spectrum with the Hydrogen Epoch of Reionization Array (HERA), and of the subhalo mass function with the Vera Rubin Observatory.

For both observable effects, the full velocity distribution of the DM is of critical relevance. The DM-SM scattering cross section responsible for the drag effect scales like v^{-4} and depends strongly on the low-velocity part of the distribution, while the suppressed growth of structure is sensitive to DM in the high-velocity tail of the distribution. In this work, we use the phase space derived in Ref. [52] which is highly nonthermal at production, although the distribution could become thermal prior to recombination through DM-DM interactions. Here we consider both the nonthermal and thermalized phase space, which bookend the range of intermediate possibilities. Our results are summarized in Fig. 1.

We note that in addition to the cosmological bounds in Fig. 1, there are stellar cooling constraints on charged particles with mass below $\mathcal{O}(10)$ keV [32,33]. However, these analyses are based on analytic estimates with a number of simplifying assumptions, and above $\sim$10 keV, the constraints are *exponentially* sensitive to assumed stellar properties. There are also ways to model build around stellar constraints [53,54]. The cosmological probes give a complementary approach, and have significant room to explore new parameter space beyond current constraints, as shown in Fig. 1.

Particle properties.—Throughout this work we assume that DM is a Dirac fermion and focus on the keV–MeV range for the DM mass, m_χ. We assume that the DM couples to the SM photon, either (i) at the level of the Lagrangian with coupling strength eQ or (ii) effectively through an ultralight (sub-eV) dark vector portal, A', where eQ is the product of the dark $U(1)'$ gauge coupling g_χ and the kinetic mixing parameter κ.

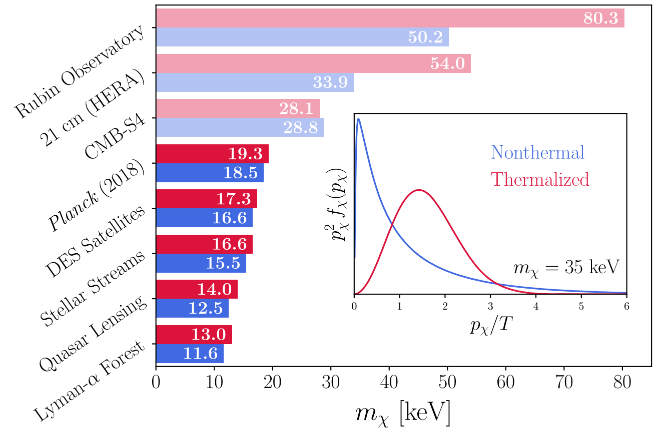

FIG. 1. Cosmological 95% bounds on DM that is produced by freeze-in through a vector mediator. Dark shaded bars correspond to excluded DM masses while light ones correspond to projected future reach. These differ depending on whether the DM phase space remains nonthermal (blue) or thermalizes through self-scattering (red). Inset: the DM phase space.

In the keV–MeV mass range, two channels are dominantly responsible for the production of DM: electron-positron annihilation $e^+e^- \to \chi\bar{\chi}$ and plasmon decays $\gamma^* \to \chi\bar{\chi}$. In the absence of additional interactions, DM will *not* be produced efficiently in the very early universe for small SM-DM couplings. We therefore assume a negligible initial abundance of DM. For freeze-in production of DM, it is possible to semi-analytically solve the Boltzmann equation, $\partial f_\chi/\partial t - H(p_\chi^2/E_\chi)\partial f_\chi/\partial E_\chi = C[f_e, f_{\gamma^*}]/E_\chi$, for the DM phase space f_χ. The collision term C does not depend on f_χ to very good approximation due to the small DM number density. In Ref. [52], we integrated this equation to find the DM phase-space distribution from freeze-in. The typical DM momentum is of order the photon temperature (see Fig. 1) since the DM inherits the kinematic properties of the plasma from which it is born. The relic DM abundance, which we assume is entirely produced by freeze-in, is determined by the 0th moment of the Boltzmann equation. This uniquely determines the effective charge Q for a given DM mass, with $Q \sim 10^{-11}$ for the range of masses considered here. We note that the limits described in this Letter do not apply for arbitrary Q and m_χ. For instance, if Q is too large, DM would be overproduced by freeze-in. Additional model features would be required to subsequently deplete the DM abundance, which would impact the phase space and cosmological observables.

After the DM is produced, DM-DM self-scattering can potentially redistribute the phase space. In our analysis, we consider two limiting cases for the DM phase-space distribution: (i) the fully nonthermal primordial phase space and (ii) a Gaussian phase space for DM that has thermalized within its own isolated sector through DM-DM interactions, which leads to a temperature T_χ that preserves

$\langle p_\chi^2 \rangle$ (assuming thermalization occurs while the DM is nonrelativistic). The first case occurs if the mediator is the SM photon, since self-scattering would be highly suppressed as Q^4. If the mediator is a dark photon, DM-DM scattering scales as g_χ^4 and thermalization can occur more efficiently. DM self-thermalization requires a high value of g_χ, which can be compensated by lowering κ to give the same value of Q. Because of bounds on DM self-interactions (for instance, from merging galaxy clusters; see, e.g., Ref. [55]), g_χ cannot be too large. However, freeze-in DM can potentially self-thermalize as early as redshift $z \sim 10^6$ without violating self-interaction bounds [52]. Because thermalization is not instantaneous, a given value of g_χ implies some time-dependent DM phase space. The bounds we present are meant to serve as endpoints of the parameter space, while in the intermediate regime there may be other effective descriptions of the phase space [56].

Baryon dragging.—The portal responsible for making DM implies a DM-baryon scattering cross section scaling as v^{-4}, which results in a drag force between the DM and the photon-baryon fluids. The drag force introduces extra damping in the amplitude of acoustic oscillations. There is also a slight suppression in the matter power spectrum for modes that are inside the horizon while the drag is active, but this does not add significant constraining power compared to the effect of the high-velocity DM phase space, which we explore in the next section.

We calculate the effects of DM-baryon drag on the CMB, shown in Fig. 2, using a modified version of the Boltzmann solver CAMB [57,58] with additional terms in the Boltzmann equations. Further details are given in the Supplemental Material [59]. We conservatively assume DM only scatters with protons and neglect DM-helium and DM-electron scattering; DM-helium drag is smaller because of earlier helium recombination, while DM-electron drag is suppressed due to the high thermal velocity of electrons. The drag enhances the first acoustic peak in the CMB and suppresses higher-ℓ fluctuations (which drive the constraints). For freeze-in, the high-velocity DM phase space leads to a smaller drag rate and correspondingly smaller δC_ℓ compared to DM with the same couplings and unphysical cold initial conditions. Among the freeze-in thermal histories, the nonthermal case has more low-velocity DM particles, resulting in larger drag rate and δC_ℓ than the thermalized case.

We set constraints by running a Markov chain Monte Carlo likelihood analysis, using CMB temperature, polarization, and lensing data from the *Planck* 2018 release [63]. For fixed DM mass, we vary the six standard ΛCDM parameters in addition to the normalization of the DM-baryon drag. The lower bound on the freeze-in mass is determined by interpolating the constraints on DM-baryon drag for a few masses, and finding where the normalization matches that of freeze-in. The primary degeneracy with

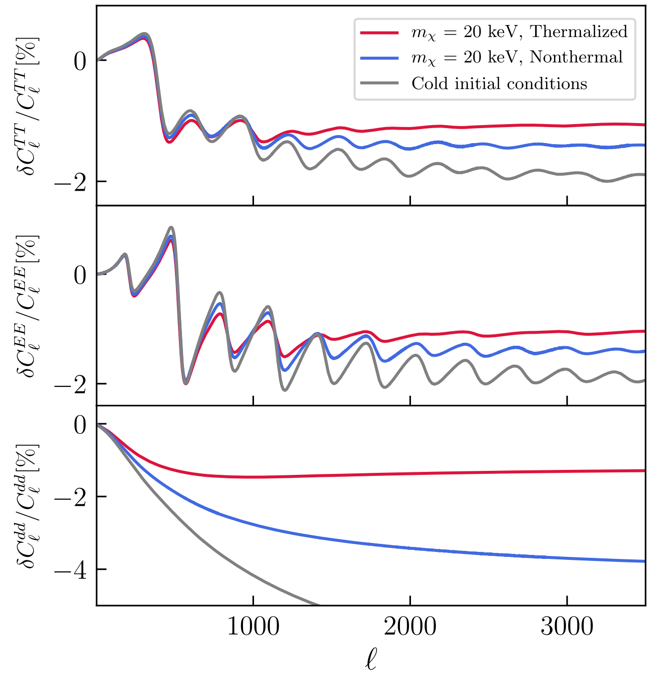

FIG. 2. Effect of DM-baryon drag on CMB temperature, polarization, and lensing power spectra. We show freeze-in DM with mass of 20 keV for different thermal histories. We also show the effect for DM that has the cross section relevant for freeze-in but with unphysical cold initial conditions (i.e., $T_\chi \to 0$), which is most similar to previous studies [60–62].

ΛCDM is with the scalar spectral index n_s, since changing n_s also results in a suppression of the acoustic peaks at high ℓ. This degeneracy is slightly larger for the nonthermal case, which is why we find a weaker *Planck* constraint despite the larger δC_ℓ.

To project the sensitivity of the future CMB-S4 experiment [64], we perform Fisher forecasts with the unlensed CMB TT, EE, and TE spectra in addition to the lensing deflection spectrum dd. Assuming that CMB-S4 can be combined with *Planck* data, we take a minimum multipole $\ell_{\min} = 30$ and impose a prior on the optical depth $\tau = 0.06 \pm 0.01$. We take a fractional sky coverage of $f_{\rm sky} = 0.4$, a maximum multipole of $\ell_{\max} = 5000$ for temperature and polarization (except for TT where $\ell_{\max} = 3000$) and $\ell_{\max} = 2500$ for lensing. We consider noise levels corresponding to a beam resolution of $\theta_{\rm FWHM} =$ 1 arcmin and a noise temperature of 1 μK-arcmin in temperature and $\sqrt{2}$ μK-arcmin in polarization. For the lensing power spectrum C_ℓ^{dd}, the noise curves are obtained from a procedure of iterative delensing using E modes and B modes [64]. CMB lensing reduces the degeneracy with n_s and provides additional constraining power on the nonthermal case, which is the primary factor that drives the stronger forecast compared to the thermal case: lensing is more powerful in constraining DM-baryon scattering at higher

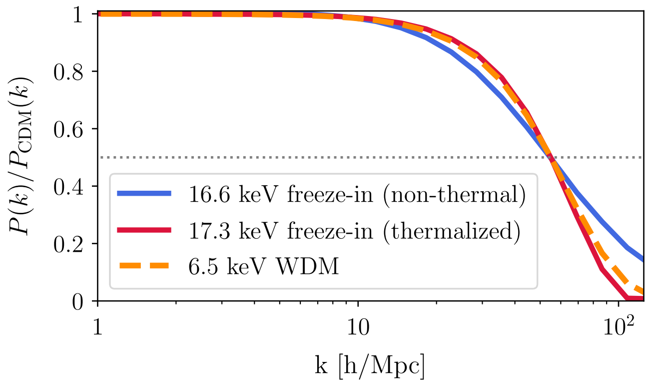

FIG. 3. Suppression of the linear matter power spectrum relative to CDM, for different DM thermal histories. For the WDM case, we show a mass of 6.5 keV which corresponds to the current strongest limits from DES [69]. For the freeze-in scenarios, we show DM masses that match the WDM power spectrum at the scale where power is suppressed by half.

redshifts [61,65], which is larger in the nonthermal case. In the primary CMB, DM-baryon drag is mildly degenerate with beyond-ΛCDM parameters, for instance, massive neutrinos and $N_{\rm eff}$; this degeneracy will be broken by future measurements of CMB lensing.

Beyond the CMB, DM-baryon drag with a scattering cross section $\propto v^{-4}$ has been proposed to explain an anomalous 21 cm absorption trough seen in EDGES [29], and could be searched for with the 21 cm power spectrum [66,67]. However, for freeze-in, we constrain the cross section to be too small to explain the absorption seen in EDGES [30], and it would also be challenging to see in the 21 cm power spectrum [67].

Effect on clustering.—The kinematics of sub-MeV freeze-in DM is inherited from relativistic electron-positron pairs and plasmons. The resulting high-speed phase-space distribution leads to a suppression in gravitational clustering on small scales, as shown in Fig. 3. The exact clustering behavior depends on whether the DM retains its nonthermal phase-space distribution. For the case where DM self-thermalizes and obtains a temperature T_χ, the suppression can be characterized by an effective sound speed for the DM fluid, $c_\chi^2 = 5T_\chi/3m_\chi$. We calculate the matter power spectrum using the fluid equations given in the Supplemental Material [59], and implemented in CAMB. For the nonthermal phase space, the suppression arises due to free-streaming and cannot be described by fluid equations. In this case, we compute the transfer functions for the linear matter power spectrum using the Boltzmann code CLASS [68], treating the DM as a massive neutrino species with the phase space for freeze-in. For either thermal history, the suppression of clustering occurs on scales that are in the nonlinear regime at present day, implying that simulations are required to study the effects, as described below.

A variety of astrophysical systems would be sensitive to suppressed clustering due to freeze-in. To determine the limits shown in Fig. 1, we compare the freeze-in transfer functions to those of warm DM (WDM), where DM is a thermal relic that decouples while relativistic. Fitting forms for the transfer functions are presented in the Supplemental Material [59]. We match the freeze-in transfer function with the WDM transfer function at the half-mode scale, $\lambda_{1/2}$, where the power spectrum is suppressed by half compared to CDM as shown in Fig. 3. For WDM initial conditions, in order to saturate the DM relic abundance the DM temperature at decoupling is $T_{\rm WDM} = 0.16 \times (1\ {\rm keV}/m_{\rm WDM})^{1/3} T_\gamma$ [note that this temperature difference requires $\mathcal{O}(10^3)$ degrees of freedom in the early universe, but the entire SM has only 106.75] whereas DM produced by freeze-in has a higher effective temperature. We therefore find that the half-mode scale for freeze-in at a given mass matches that of WDM with a smaller mass. Freeze-in DM that self-thermalizes yields a transfer function that almost exactly matches WDM for the appropriate choice of masses, and we therefore rest our analysis on existing simulations of WDM. However, there is a difference in the shape of the transfer function for the nonthermal case, which has a larger high-velocity tail. We consider limits on the nonthermal case to be estimates, and expect that more accurate limits can be obtained by accounting for the full transfer function in dedicated simulations.

The Lyman-α forest of quasar spectral absorption lines is sensitive to clustering on $k \sim 10\ h/{\rm Mpc}$ scales. We use the limit $m_{\rm WDM} > 5.3$ keV from Ref. [70] which analyzed data from XQ-100 [71] and HIRES/MIKE [72] in tandem with hydrodynamical simulations. References [73,74] found a similar constraint from the combined analysis of data from XQ-100, HIRES/MIKE, and the Baryon Oscillation Spectroscopic Survey of the Sloan Digital Sky Survey (SDSS) [75]. For the nonthermal freeze-in history, we follow Ref. [76], which studied the effect of various DM transfer function shapes on Lyman-α flux power spectra. For fixed half-mode scale, power spectra with a shallower decline are more readily rejected by analyses of the Lyman-α forest than steeper counterparts [76]. It is therefore conservative to set a limit on the nonthermal case by matching the half-mode scale. Based on improved recent constraints on the ultralight DM transfer function [77,78] from the Lyman-α forest [79], we estimate that a constraint on freeze-in of $m_\chi \sim 30$ keV can be set in the near future with similar methods.

The abundance of DM halos and subhalos also inherits any small-scale suppression in the matter power spectrum. In particular, the half-mode scale $\lambda_{1/2}$ translates to a halo mass scale $M_{1/2} = \pi\lambda_{1/2}^3\bar{\rho}_m/6$. The halo and subhalo mass functions would be suppressed for masses below $M_{1/2}$, meaning that the existence of low-mass subhalos excludes WDM below some particle mass scale. These bounds are determined by simulation and astrophysical uncertainties must be treated with care, as expounded on in the references below. Based on the population of classical and SDSS-discovered MW satellites, the constraint is

$m_{\mathrm{WDM}} > 3.3$ keV [80]. The discovery of MW satellites by DES and Pan-STARRS (PS) strengthens this constraint to $m_{\mathrm{WDM}} > 6.5$ keV [69]. Strong gravitational lensing of quadruply imaged quasars by foreground galaxies provides further evidence for an abundance of subhalos, which affect the flux ratios and positions of the images. Analyses of such systems constrain $m_{\mathrm{WDM}} > 5.6$ keV [81] (see also Ref. [82]). Combining these independent probes of structure formation can further improve the bound [83,84]; with the recent limit of $m_{\mathrm{WDM}} > 9.7$ keV [84], it may be possible to extend the constraint on freeze-in up to 25–30 keV. Low-mass subhalos can also perturb the densities of stellar streams in a characteristic way, leaving gaps that can persist on Gyr timescales. Based on PS and *Gaia* observations of GD-1 and Pal 5, there is evidence for DM substructure [85,86]; when combined with classical MW satellite abundances, stellar streams constrain $m_{\mathrm{WDM}} > 6.3$ keV.

In the future, measurements of the 21 cm absorption signal from cosmic dawn will be sensitive to the properties of low-mass halos. Nonstandard small-scale structure formation would affect the star formation history and leave an imprint on the 21 cm power spectrum as seen by HERA, and WDM masses up to $m_{\mathrm{WDM}} \sim 14$ keV could be constrained in the near future [87]. Additionally, a target of the Rubin Observatory is to probe $m_{\mathrm{WDM}} \sim 18$ keV by probing the subhalo mass function down to masses of $10^6\ \mathrm{M}_\odot$ [88].

Finally, the phase space density in dwarf spheroidal galaxies can used to constrain freeze-in, see, e.g., Ref. [89] and references therein. The strongest bounds generally come from applying Liouville's theorem, whereby the maximum phase space density in a dwarf spheroidal cannot exceed the primordial value assuming collisionless evolution. However, the maximum primordial phase space density for freeze-in (both in the thermalized and nonthermal cases) is higher than what is found in dwarf galaxies, meaning there is no constraint on freeze-in for keV-scale masses. Another phase space limit comes from the Pauli exclusion principle and requiring that the Fermi velocity of a dwarf galaxy consisting of a degenerate Fermi gas not exceed the escape velocity [90]. A recent application of this idea finds $m > 0.13$ keV [89].

Conclusions.—Sub-MeV freeze-in via a light vector mediator sits at the nexus of many interesting possible DM properties. Freeze-in is the only minimal way to make charged DM and is one of very few ways to make sub-MeV DM from a SM thermal process in the early universe. These properties, combined with a predictive direct-detection signal in the light-mediator regime, make freeze-in a key benchmark for proposed sub-MeV direct-detection experiments. This DM candidate is dominantly born from the decay of plasmons and has a nonthermal, high-velocity phase-space distribution, making it behave like WDM. Based on observations of clustering on small scales, we have excluded freeze-in masses below ∼17 keV. This DM candidate can also scatter with baryons in the primordial plasma, altering the CMB and allowing us to exclude freeze-in masses below ∼19 keV. In the near future, cosmological probes have substantial room for improvement and will test freeze-in masses up to almost 100 keV, greatly complementing terrestrial efforts to directly detect sub-MeV DM.

We thank Asher Berlin, Steen Hansen, Adrian Liu, Pat McDonald, Julian Muñoz, Keir Rogers, Tracy R. Slatyer, and Linda Xu for useful conversations pertaining to this work. C. D. was partially supported by NSF Grant No. AST-1813694. T. L. is supported by an Alfred P. Sloan Foundation fellowship and the Department of Energy under Grant No. DE-SC0019195. K. S. was supported by a Pappalardo Fellowship in the MIT Department of Physics and by NASA through the NASA Hubble Fellowship Grant No. HST-HF2-51470.001-A awarded by the Space Telescope Science Institute, which is operated by the Association of Universities for Research in Astronomy, Incorporated, under NASA Contract No. NAS5-26555. K. S. also acknowledges support from the National Science Foundation and the Hertz Foundation during early stages of this work.

*cdvorkin@g.harvard.edu
†tongyan@physics.ucsd.edu
‡kschutz@mit.edu

[1] T. Asaka, K. Ishiwata, and T. Moroi, Phys. Rev. D **73**, 051301(R) (2006).
[2] T. Asaka, K. Ishiwata, and T. Moroi, Phys. Rev. D **75**, 065001 (2007).
[3] S. Gopalakrishna, A. de Gouvea, and W. Porod, J. Cosmol. Astropart. Phys. 05 (2006) 005.
[4] V. Page, J. High Energy Phys. 04 (2007) 021.
[5] L. J. Hall, K. Jedamzik, J. March-Russell, and S. M. West, J. High Energy Phys. 03 (2010) 080.
[6] N. Bernal, M. Heikinheimo, T. Tenkanen, K. Tuominen, and V. Vaskonen, Int. J. Mod. Phys. A **32**, 1730023 (2017).
[7] R. Essig, J. Mardon, and T. Volansky, Phys. Rev. D **85**, 076007 (2012).
[8] R. Essig, A. Manalaysay, J. Mardon, P. Sorensen, and T. Volansky, Phys. Rev. Lett. **109**, 021301 (2012).
[9] R. Essig, M. Fernandez-Serra, J. Mardon, A. Soto, T. Volansky, and T.-T. Yu, J. High Energy Phys. 05 (2016) 046.
[10] Y. Hochberg, Y. Kahn, M. Lisanti, C. G. Tully, and K. M. Zurek, Phys. Lett. B **772**, 239 (2017).
[11] S. Derenzo, R. Essig, A. Massari, A. Soto, and T.-T. Yu, Phys. Rev. D **96**, 016026 (2017).
[12] Y. Hochberg, Y. Kahn, M. Lisanti, K. M. Zurek, A. G. Grushin, R. Ilan, S. M. Griffin, Z.-F. Liu, S. F. Weber, and J. B. Neaton, Phys. Rev. D **97**, 015004 (2018).
[13] S. Knapen, T. Lin, M. Pyle, and K. M. Zurek, Phys. Lett. B **785**, 386 (2018).
[14] S. Griffin, S. Knapen, T. Lin, and K. M. Zurek, Phys. Rev. D **98**, 115034 (2018).
[15] K. Schutz and K. M. Zurek, Phys. Rev. Lett. **117**, 121302 (2016).

[16] S. Knapen, T. Lin, and K. M. Zurek, Phys. Rev. D **95**, 056019 (2017).
[17] Y. Hochberg, Y. Zhao, and K. M. Zurek, Phys. Rev. Lett. **116**, 011301 (2016).
[18] Y. Hochberg, M. Pyle, Y. Zhao, and K. M. Zurek, J. High Energy Phys. 08 (2016) 057.
[19] Y. Hochberg, I. Charaev, S.-W. Nam, V. Verma, M. Colangelo, and K. K. Berggren, Phys. Rev. Lett. **123**, 151802 (2019).
[20] N. A. Kurinsky, T. C. Yu, Y. Hochberg, and B. Cabrera, Phys. Rev. D **99**, 123005 (2019).
[21] S. M. Griffin, K. Inzani, T. Trickle, Z. Zhang, and K. M. Zurek, Phys. Rev. D **101**, 055004 (2020).
[22] A. Coskuner, A. Mitridate, A. Olivares, and K. M. Zurek, Phys. Rev. D **103**, 016006 (2021).
[23] R. M. Geilhufe, F. Kahlhoefer, and M. W. Winkler, Phys. Rev. D **101**, 055005 (2020).
[24] A. Berlin, R. T. D'Agnolo, S. A. R. Ellis, P. Schuster, and N. Toro, Phys. Rev. Lett. **124**, 011801 (2020).
[25] S. M. Griffin, Y. Hochberg, K. Inzani, N. Kurinsky, T. Lin, and T. C. Yu, Phys. Rev. D **103**, 075002 (2021).
[26] S. Knapen, T. Lin, and K. M. Zurek, Phys. Rev. D **96**, 115021 (2017).
[27] D. Green and S. Rajendran, J. High Energy Phys. 10 (2017) 013.
[28] S. D. McDermott, H.-B. Yu, and K. M. Zurek, Phys. Rev. D **83**, 063509 (2011).
[29] J. D. Bowman, A. E. E. Rogers, R. A. Monsalve, T. J. Mozdzen, and N. Mahesh, Nature (London) **555**, 67 (2018).
[30] R. Barkana, N. J. Outmezguine, D. Redigolo, and T. Volansky, Phys. Rev. D **98**, 103005 (2018).
[31] A. Berlin, D. Hooper, G. Krnjaic, and S. D. McDermott, Phys. Rev. Lett. **121**, 011102 (2018).
[32] S. Davidson, S. Hannestad, and G. Raffelt, J. High Energy Phys. 05 (2000) 003.
[33] H. Vogel and J. Redondo, J. Cosmol. Astropart. Phys. 02 (2014) 029.
[34] J. H. Chang, R. Essig, and S. D. McDermott, J. High Energy Phys. 09 (2018) 051.
[35] A. Bhoonah, J. Bramante, F. Elahi, and S. Schon, Phys. Rev. D **100**, 023001 (2019).
[36] D. Wadekar and G. R. Farrar, Phys. Rev. D **103**, 123028 (2021).
[37] L. Ackerman, M. R. Buckley, S. M. Carroll, and M. Kamionkowski, Phys. Rev. D **79**, 023519 (2009).
[38] M. Heikinheimo, M. Raidal, C. Spethmann, and H. Veermäe, Phys. Lett. B **749**, 236 (2015).
[39] A. Stebbins and G. Krnjaic, J. Cosmol. Astropart. Phys. 12 (2019) 003.
[40] J.-T. Li and T. Lin, Phys. Rev. D **101**, 103034 (2020).
[41] D. Dunsky, L. J. Hall, and K. Harigaya, J. Cosmol. Astropart. Phys. 07 (2019) 015.
[42] R. Lasenby, J. Cosmol. Astropart. Phys. 11 (2020) 034.
[43] S. A. Abel, M. D. Goodsell, J. Jaeckel, V. V. Khoze, and A. Ringwald, J. High Energy Phys. 07 (2008) 124.
[44] M. Goodsell, J. Jaeckel, J. Redondo, and A. Ringwald, J. High Energy Phys. 11 (2009) 027.
[45] S. Davidson, S. Hannestad, and G. Raffelt, J. High Energy Phys. 05 (2000) 003.
[46] X.-D. Shi and G. M. Fuller, Phys. Rev. Lett. **82**, 2832 (1999).
[47] A. Berlin and N. Blinov, Phys. Rev. Lett. **120**, 021801 (2018).
[48] C. Boehm, M. J. Dolan, and C. McCabe, J. Cosmol. Astropart. Phys. 08 (2013) 041.
[49] K. M. Nollett and G. Steigman, Phys. Rev. D **89**, 083508 (2014).
[50] N. Sabti, J. Alvey, M. Escudero, M. Fairbairn, and D. Blas, J. Cosmol. Astropart. Phys. 01 (2020) 004.
[51] H. An, M. Pospelov, and J. Pradler, Phys. Lett. B **725**, 190 (2013).
[52] C. Dvorkin, T. Lin, and K. Schutz, Phys. Rev. D **99**, 115009 (2019).
[53] A. E. Nelson and J. Walsh, Phys. Rev. D **77**, 095006 (2008).
[54] W. DeRocco, P. W. Graham, and S. Rajendran, Phys. Rev. D **102**, 075015 (2020).
[55] S. Tulin and H.-B. Yu, Phys. Rep. **730**, 1 (2018).
[56] R. Huo, Phys. Lett. B **802**, 135251 (2020).
[57] A. Lewis, A. Challinor, and A. Lasenby, Astrophys. J. **538**, 473 (2000).
[58] C. Howlett, A. Lewis, A. Hall, and A. Challinor, J. Cosmol. Astropart. Phys. 04 (2012) 027.
[59] See Supplemental Material at http://link.aps.org/supplemental/10.1103/PhysRevLett.127.111301 for further details regarding the modified Boltzmann equations that include baryon dragging effects, the constraints obtained from the Planck 2018 likelihoods, the Fisher forecasts for CMB-S4, the fitting forms for the freeze-in transfer functions, the effects of baryon drag on the matter power spectrum, and the dark photon parameter space for freeze-in.
[60] C. Dvorkin, K. Blum, and M. Kamionkowski, Phys. Rev. D **89**, 023519 (2014).
[61] K. K. Boddy, V. Gluscevic, V. Poulin, E. D. Kovetz, M. Kamionkowski, and R. Barkana, Phys. Rev. D **98**, 123506 (2018).
[62] T. R. Slatyer and C.-L. Wu, Phys. Rev. D **98**, 023013 (2018).
[63] N. Aghanim *et al.* (Planck Collaboration), Astron. Astrophys. **641**, A5 (2020).
[64] K. N. Abazajian *et al.* (CMB-S4 Collaboration), arXiv:1610.02743.
[65] Z. Li, V. Gluscevic, K. K. Boddy, and M. S. Madhavacheril, Phys. Rev. D **98**, 123524 (2018).
[66] J. B. Muñoz, E. D. Kovetz, and Y. Ali-Haïmoud, Phys. Rev. D **92**, 083528 (2015).
[67] J. B. Muñoz, C. Dvorkin, and A. Loeb, Phys. Rev. Lett. **121**, 121301 (2018).
[68] D. Blas, J. Lesgourgues, and T. Tram, J. Cosmol. Astropart. Phys. 07 (2011) 034.
[69] E. Nadler *et al.* (DES Collaboration), Phys. Rev. Lett. **126**, 091101 (2021).
[70] V. Iršič *et al.*, Phys. Rev. D **96**, 023522 (2017).
[71] S. López, V. D'Odorico, S. Ellison, G. Becker, L. Christensen, G. Cupani, K. Denney, I. Pâris, G. Worseck, T. Berg *et al.*, Astron. Astrophys. **594**, A91 (2016).
[72] M. Viel, G. D. Becker, J. S. Bolton, and M. G. Haehnelt, Phys. Rev. D **88**, 043502 (2013).
[73] C. Yèche, N. Palanque-Delabrouille, J. Baur, and H. du Mas des Bourboux, J. Cosmol. Astropart. Phys. 06 (2017) 047.

[74] J. Baur, N. Palanque-Delabrouille, C. Yeche, A. Boyarsky, O. Ruchayskiy, É. Armengaud, and J. Lesgourgues, J. Cosmol. Astropart. Phys. 12 (2017) 013.
[75] N. Palanque-Delabrouille *et al.*, Astron. Astrophys. **559**, A85 (2013).
[76] R. Murgia, V. Iršič, and M. Viel, Phys. Rev. D **98**, 083540 (2018).
[77] W. Hu, R. Barkana, and A. Gruzinov, Phys. Rev. Lett. **85**, 1158 (2000).
[78] R. Hložek, D. J. E. Marsh, D. Grin, R. Allison, J. Dunkley, and E. Calabrese, Phys. Rev. D **95**, 123511 (2017).
[79] K. K. Rogers and H. V. Peiris, Phys. Rev. Lett. **126**, 071302 (2021).
[80] E. O. Nadler, V. Gluscevic, K. K. Boddy, and R. H. Wechsler, Astrophys. J. **878**, L32 (2019); Astrophys. J. Lett. **878**, L32 (2019).
[81] J.-W. Hsueh, W. Enzi, S. Vegetti, M. Auger, C. D. Fassnacht, G. Despali, L. V. Koopmans, and J. P. McKean, Mon. Not. R. Astron. Soc. **492**, 3047 (2020).
[82] D. Gilman, S. Birrer, A. Nierenberg, T. Treu, X. Du, and A. Benson, Mon. Not. R. Astron. Soc. **491**, 6077 (2020).
[83] W. Enzi *et al.*, arXiv:2010.13802.
[84] E. O. Nadler, S. Birrer, D. Gilman, R. H. Wechsler, X. Du, A. Benson, A. M. Nierenberg, and T. Treu, arXiv:2101.07810.
[85] N. Banik, J. Bovy, G. Bertone, D. Erkal, and T. J. L. de Boer, Mon. Not. R. Astron. Soc. **502**, 2364 (2021).
[86] N. Banik, J. Bovy, G. Bertone, D. Erkal, and T. J. L. de Boer, arXiv:1911.02663.
[87] J. B. Muñoz, C. Dvorkin, and F.-Y. Cyr-Racine, Phys. Rev. D **101**, 063526 (2020).
[88] A. Drlica-Wagner *et al.* (LSST Dark Matter Group), arXiv:1902.01055.
[89] J. Alvey, N. Sabti, V. Tiki, D. Blas, K. Bondarenko, A. Boyarsky, M. Escudero, M. Fairbairn, M. Orkney, and J. I. Read, Mon. Not. R. Astron. Soc. **501**, 1188 (2020).
[90] S. Tremaine and J. E. Gunn, Phys. Rev. Lett. **42**, 407 (1979).